analytical chemistry

Article

pubs.acs.org/ac

Application of Adenosine Triphosphate Affinity Probe and Scheduled Multiple-Reaction Monitoring Analysis for Profiling Global Kinome in Human Cells in Response to Arsenite Treatment

Lei Guo,[†] Yongsheng Xiao,[‡] and Yinsheng Wang*[,†,‡]

[†]Environmental Toxicology Graduate Program and [‡]Department of Chemistry, University of California, Riverside, California 92521-0403, United States

Supporting Information

ABSTRACT: Phosphorylation of cellular components catalyzed by kinases plays important roles in cell signaling and proliferation. Quantitative assessment of perturbation in global kinome may provide crucial knowledge for elucidating the mechanisms underlying the cytotoxic effects of environmental toxicants. Here, we utilized an adenosine triphosphate (ATP) affinity probe coupled with stable isotope labeling by amino acids in cell culture (SILAC) to assess quantitatively the arsenite-induced alteration of global kinome in human cells. We constructed a SILAC-compatible kinome library for scheduled multiple-reaction monitoring (MRM) analysis and adopted on-the-fly recalibration of retention time shift, which provided better throughput of the analytical method and enabled the simultaneous quantification of the expression of ~300 kinases in two LC-MRM runs. With this improved analytical method, we conducted an in-depth quantitative analysis of the perturbation of kinome of GM00637 human skin fibroblast cells induced by arsenite exposure. Several kinases involved in cell cycle progression, including cyclin-dependent kinases (CDK1 and CDK4) and Aurora kinases A, B, and C, were found to be hyperactivated, and the altered expression of CDK1 was further validated by Western analysis. In addition, treatment with a CDK inhibitor, flavopiridol, partially restored the arsenite-induced growth inhibition of human skin fibroblast cells. Thus, sodium arsenite may confer its cytotoxic effect partly through the aberrant activation of CDKs and the resultant perturbation of cell cycle progression. Together, we developed a high-throughput, SILAC-compatible, and MRM-based kinome profiling method and demonstrated that the method is powerful in deciphering the molecular modes of action of a widespread environmental toxicant. The method should be generally applicable for uncovering the cellular pathways triggered by other extracellular stimuli.

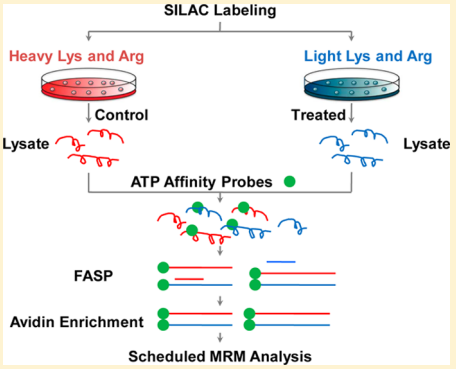

As one of the most important family of enzymes, kinases are extensively engaged in numerous cellular pathways, from metabolism to signal transduction.[1] The kinase-mediated phosphorylation of proteins, lipids, and carbohydrates controls the activation/deactivation, cellular localization, binding affinity, and degradation of the substrate molecules.[2] Thus, regulation of the function and localization of kinases is the foundation to maintain proper cell proliferation, differentiation, and apoptosis, while aberrant regulation of kinases may lead to the induction of diseases and development of tumors.[3] Along this line, the perturbation of the cellular phosphorylation pattern by modulating kinases is one of the primary deleterious effects exerted by environmental toxicants.[4] Thus, a thorough assessment of the alterations of the expression and activity of the entire kinome, which refers to the collection of global kinases, is vital for understanding the modes of action of various environmental toxicants and for exploiting effective therapeutic interventions against toxicant exposure.

Efforts have been made into exploring effective strategies to interrogate the expression and activation of kinases. Conventional immunoanalysis with kinase/phospho-specific antibodies or peptide chips has provided information on the regulation and enzymatic activities of individual or specific groups of kinases.[5,6] However, these strategies are restricted by the specificity and availability of kinase antibodies or substrates. Recent advances in mass spectrometry (MS) instrumentation, along with the development of bioinformatic tools, have led to great success in the identification and quantification of global proteome and phosphoproteome.[7,8] However, since kinases are of relatively low abundance, interference from highly abundant proteins hampers the detection of kinases, rendering the studies of global kinome by MS very challenging. Therefore, it would be highly beneficial to apply efficient kinase enrichment steps prior to MS analysis. To this end, the kinase inhibitor-based enrichment method[9] and biotin-conjugated acyl nucleotide probe affinity assay,[10,11] coupled with LC-MS/MS analysis in the data-dependent acquisition (DDA) mode, have facilitated high-throughput characterizations of the global kinome from whole cell lysates or tissue extracts. However, in the DDA mode, where 10−20 of the most abundant precursor ions are

Received: July 14, 2014
Accepted: October 9, 2014
Published: October 9, 2014

   dx.doi.org/10.1021/ac502592d | *Anal. Chem.* 2014, 86, 10700−10707

selected for fragmentation to achieve peptide identification,[12] the sensitivity and reproducibility for kinase discovery is limited by the complexity of samples and variations in precursor ion selection. Recently, with the application of the triple quadrupole mass spectrometer and advances in software development for multiple-reaction monitoring (MRM) analysis,[13,14] a targeted quantification method has gained advantages over the above-mentioned discovery-based approach in terms of sensitivity, quantification accuracy, and reproducibility.[15]

We recently constructed an MRM kinome library consisting of ~400 strictly selected peptides representing more than 300 unique kinases based on data acquired in DDA mode on an LTQ Orbitrap Velos mass spectrometer.[13] With the use of the MRM kinome library, together with the application of a desthiobiotin-based isotope-coded adenosine triphosphate (ATP)-affinity probe (ICAP) for kinase labeling, kinase peptide enrichment, and LC-MS/MS analysis on a triple quadrupole mass spectrometer, we were able to reproducibly identify and quantify more than ~250 protein and lipid kinases in cancer cells and tissues.[13] In this highly multiplexed detection, it is essential to perform scheduled MRM analysis where the mass spectrometer is programmed to detect only a limited number of peptides in predefined retention time windows. To achieve that, we calculated the "iRT" score[16] for each targeted kinase peptide to accurately predict its retention time in scheduled MRM analysis. In our previous workflow, the global kinome profiling was achieved by monitoring ~2000 transitions in 4 LC-MRM runs with the duration of retention time window being set at 10 min. We used a relatively wide retention time window in our previous study mainly due to the observed retention time shift between sequential LC-MS/MS runs; although the elution order of peptides strictly follows the iRT scales, a systematic retention time shift of peptides was observed possibly due to sample loading. To correct for retention time shift, here, we adopted "on-the-fly" recalibration[16,17] of retention time shift with spiked-in reference peptides in the targeted kinome analysis. With the increased accuracy in retention time prediction, we were able to shorten the retention time window of our scheduled MRM analysis to 6 min, thereby enabling the monitoring of the same number of transitions within two LC-MS/MS runs without compromising the overall analytical performance.

By coupling stable isotope labeling by amino acids in cell culture (SILAC)[18−20] with the ATP-affinity probe in the targeted quantitative kinome analysis for the first time, we achieved an in-depth analysis of inorganic As(III)-induced global kinome perturbation in GM00637 human skin fibroblasts. We were able to quantify 234 kinases from one forward and two reverse SILAC labeling experiments. Among them, 8 and 9 kinases were found to be significantly decreased and increased, respectively, in protein expression level and ATP binding activity. To the best of our knowledge, this is the first report about the investigation of global human kinome response under exposure to an environmental toxicant. Moreover, we demonstrated that the targeted MRM-based kinome analysis is amenable to both chemical and metabolic labeling and is a powerful tool in the exploration of the disturbance in cellular signaling network after external stimuli.

METHODS

Cell Culture. All reagents unless otherwise stated were purchased from Sigma-Aldrich (St. Louis, MO). GM00637 human skin fibroblasts were kindly provided by Prof. Gerd P. Pfeifer (the City of Hope) and cultured at 37 °C in an atmosphere containing 5% CO_2 in Dulbecco's Modified Eagle's Media (DMEM, ATCC, Manassas, VA), supplemented with 10% fetal bovine serum (FBS, Life Technologies, Grand Island, NY) and 1% antibiotic−antimycotic solution (Life Technologies).

The MTT assay was performed using Cell Proliferation Kit 1 (Roche, Basel, Switzerland) as previously described.[21] For metabolic labeling using SILAC, GM00637 cells were cultured in DMEM media for SILAC (DMEM media minus L-lysine and L-arginine, Thermo Scientific, Waltham, MA), supplemented with light lysine and arginine, or heavy stable isotope-labeled [$^{13}C_6$,$^{15}N_2$]-L-lysine and [$^{13}C_6$]-L-arginine, following previously published procedures.[22] SILAC GM00637 cells were maintained under the same conditions as noted above, except that dialyzed FBS (Life Technologies) was used. The cells were cultured in the heavy or light medium for at least five passages prior to arsenite exposure to ensure nearly complete incorporation of the stable isotope-labeled amino acids.

Sodium Arsenite Treatment and Cell Lysis. After SILAC labeling, light and heavy-labeled GM00637 cells at a density of ~5 × 10^5 cells/mL were treated with 5 μM sodium arsenite [iAs(III)] for 24 h without dialyzed FBS in forward and reverse SILAC labeling experiments, respectively. Cells were then harvested with trypsin-EDTA solution (ATCC) and washed with ice-cold phosphate-buffered saline (PBS) for three times. The pelleted cells were lysed with 0.7% CHAPS in a solution containing 50 mM HEPES (pH 7.4), 0.5 mM EDTA, 100 mM NaCl, and a protease inhibitor cocktail (100:1). Supernatant was then collected after centrifugation at 16 000g for 30 min, and the total protein concentration was determined by a Bicinchoninic Acid Kit for Protein Determination. The light-labeled, iAs(III)-treated cell lysate was mixed with the heavy-labeled, control cell lysate at a 1:1 ratio (w/w) in the forward SILAC experiment. In the reverse SILAC experiment, both the labeling and iAs(III) treatment were reversed. The cell lysate mixture was further purified through Illustra NAP-25 Columns (GM Healthcare Bio-Sciences, Pittsburgh, PA) to remove endogenous nucleotides.

ATP Affinity Probe Labeling and Sample Preparation. The detailed procedures for ATP affinity probe labeling, tryptic digestion, and affinity purification of desthiobiotin-labeled peptides were reported previously.[13] Briefly, after incubation with the ATP affinity probe for 2.5 h,[11,23] the labeled cell lysate mixture was reduced with dithiothreitol, alkylated with iodoacetamide, and digested with sequencing grade trypsin (Roche Applied Science, Indianapolis, IN). The resultant desthiobiotin-labeled peptides were enriched by using avidin−agarose resin and eluted with a buffer containing 1% TFA in CH_3CN/H_2O (7:3, v/v). The resulting enriched peptide samples were desalted by employing OMIX C_{18} pipet tips (Agilent Technologies, Santa Clara, CA).

Scheduled LC-MRM Analysis and On-the-Fly Correction of Retention Time Shift. A TSQ Vantage triple-quadrupole mass spectrometer (Thermo Fisher Scientific, San Jose, CA) was utilized for the scheduled LC-MRM analysis with on-the-fly correction for retention time (RT) shift. The mass spectrometer was coupled to an EASY n-LCII HPLC system with a nanoelectrospray ionization source (Thermo Fisher Scientific). The experimental conditions for the scheduled LC-MRM analysis were described elsewhere.[13] To achieve on-the-fly recalibration of retention time shift, standard reference peptides (Pierce Peptide Retention Time Calibration Mixture,

dx.doi.org/10.1021/ac502592d | Anal. Chem. 2014, 86, 10700−10707

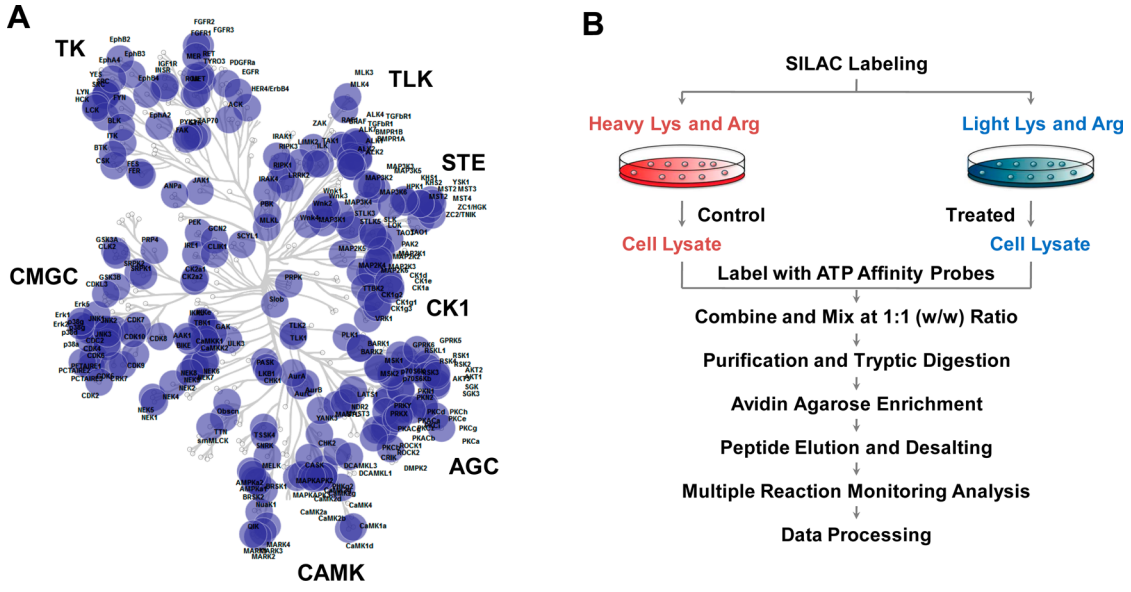

Figure 1. Targeted human kinases mapped in the dendrogram of the SILAC-compatible kinome library (A) and a general workflow of SILAC-based multiple reaction monitoring (MRM) analysis for global kinome profiling using the ATP affinity probe (B).

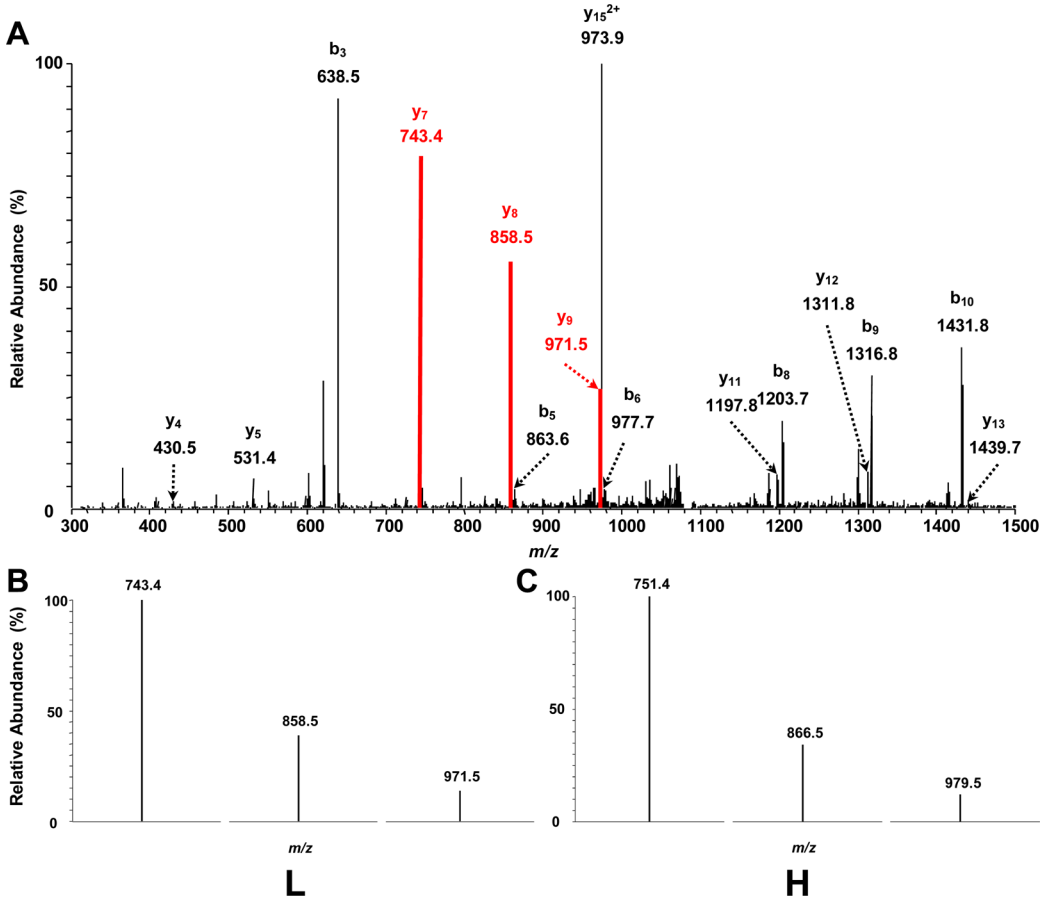

Figure 2. Representative MS/MS data revealed the reliable identification of glycogen synthase kinase-3 beta. (A) The MS/MS of glycogen synthase kinase-3 beta peptide DIK*PQNLLLDPDTAVLK ("K*" designates the desthiobiotin-labeled lysine) in the kinome library based on data-dependent analysis. (B–C) MS/MS for the same peptide from targeted analysis with light- and heavy-labeled lysine, respectively.

Thermo Fisher Scientific) with pregenerated iRT values (Table S1, Supporting Information) were spiked into samples. In the process of an LC-MRM run, the RT shift was evaluated on the basis of the RTs of the reference peptides. The RT window of the subsequent peptides was then adjusted in real time according to the linear regression of the two preceding reference peptides. Thus, the improved accuracy in RT prediction increased overall analytical robustness and allowed

dx.doi.org/10.1021/ac502592d | Anal. Chem. 2014, 86, 10700–10707

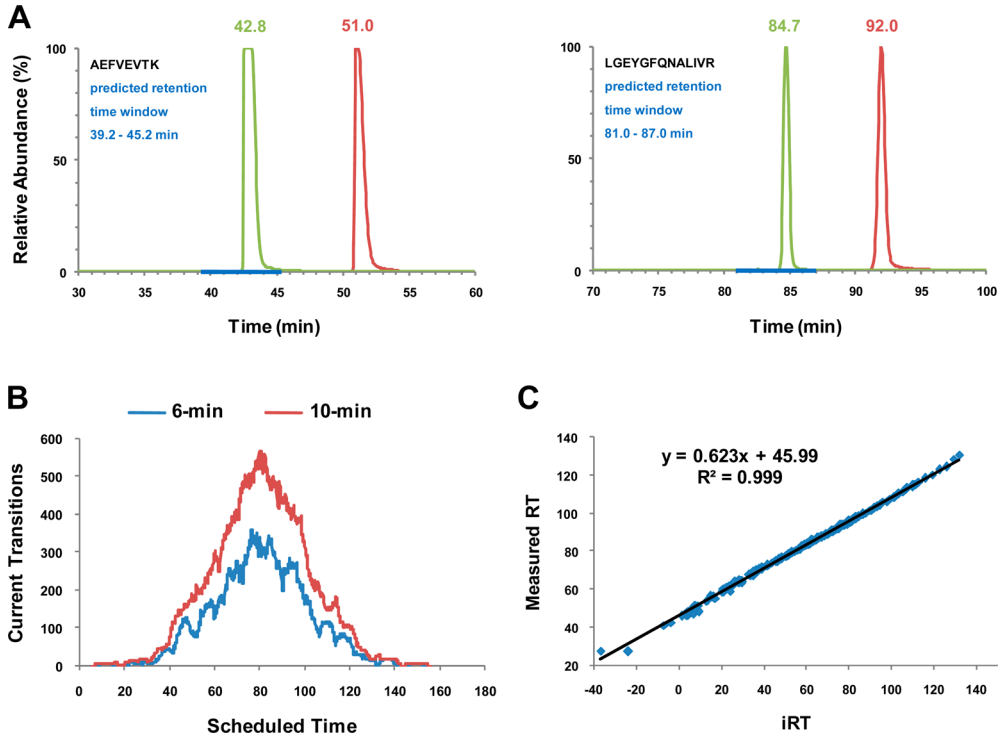

Figure 3. Proof of concept for on-the-fly retention time calibration using tryptic peptides of BSA (A, B) and linearity of calculated iRT versus measured retention time based on LC-MS/MS analysis on a TSQ Vantage mass spectrometer (C). (A) Extracted-ion chromatograms for two representative BSA peptides AEFVEVTK and LGEYGFQNALIVR from two LC-MRM analyses with different gradients. The traces acquired in the initial and intentionally delayed gradients are shown in green and red, respectively. The blue line depicts the predicted retention time window. (B) Number of transitions scheduled in each cycle with a 6 and 10 min retention time window, respectively. (C) iRT-based retention time prediction achieved a good correlation with an R^2 value of 0.999 on the measurement of 245 peptides with a 130 min linear gradient.

for the use of a shortened RT window in the scheduled MRM analysis. The retention time windows for the reference peptides (IGDYAGIK and TASEFDSAIAQDK) and the remaining peptides were set up as 16 and 6 min, respectively. Therefore, the ~2000 transitions corresponding to ~400 peptides from ~300 kinases could be monitored in two LC-MRM runs. Data were processed against the MRM-based kinome library[13] adapted for SILAC labeling on Skyline, version 1.4.0.4421.[14]

RESULTS AND DISCUSSION

Quantitative Analysis of Global Kinome by ATP Affinity Probe with SILAC Labeling. Recently, we constructed a human MRM kinome library on the basis of large-scale shotgun proteomic analysis of kinases enriched by desthiobiotin-based isotope-coded ATP affinity probes from the whole cell lysates of six different cell lines (K562, IMR-90, HeLa-S3, Jurkat-T, WM-115, and WM-266-4).[13] The acquired tandem mass spectra and retention time information on kinase-derived peptides with desthiobiotin labeling were then processed using Skyline for the MRM library construction. However, the use of isotope-coded ATP affinity probes in the previous study required customized synthesis, which may limit its general application in analytical laboratories. To accommodate for a more widely used quantitative approach using SILAC, we reconstructed the human MRM kinome library by setting up variable modifications with mass shifts introduced by heavy isotope labeling with lysine (+8 Da) and arginine (+6 Da). The current SILAC-compatible MRM kinome library consists of 395 peptides, corresponding to 285 kinases, which allows for in-depth kinome profiling that covers all the seven major human kinase families (Figure 1A).

To achieve quantitative analysis of the global kinome, we employed metabolic labeling with SILAC (Figure 1B). After complete incorporation of the light- and heavy-labeled amino acids, the cells were exposed to sodium arsenite and subsequently lysed. The light and heavy cell lysates were then incubated with ATP affinity probe, mixed at a 1:1 ratio (w/w), and digested with trypsin. After avidin agarose enrichment, the desthiobiotin-conjugated peptides were eluted and subjected to scheduled LC-MRM analysis.

Our results revealed that accurate MRM identification and quantification of SILAC-labeled human kinome can be achieved by referring to the spectra of targeted peptides in our SILAC-compatible MRM kinome library. LC-MRM results of a representative peptide DIK*PQNLLLDPDTAVLK (K* is desthiobiotin-labeled lysine) from glycogen synthase kinase-3 beta are depicted in Figure 2. On the basis of the MS/MS in the kinome library obtained from data-dependent analysis, transitions of three abundant y ions (y_7, y_8, and y_9) were selected for MRM monitoring of light- and heavy-labeled kinase peptides (Figure 2A). Subsequent MRM analysis results revealed reliable monitoring of the corresponding light and heavy forms of these three ions (Figure 2B,C). The relative abundances of the three y ions from both light- and heavy-SILAC labeled kinase peptides were consistent with those in the original spectrum in the library, confirming the unbiased identification and quantification of this peptide. Therefore, our MRM-based targeted kinome analysis is fully compatible with SILAC labeling, thereby further broadening the application of this method for global kinome profiling.

dx.doi.org/10.1021/ac502592d | Anal. Chem. 2014, 86, 10700−10707

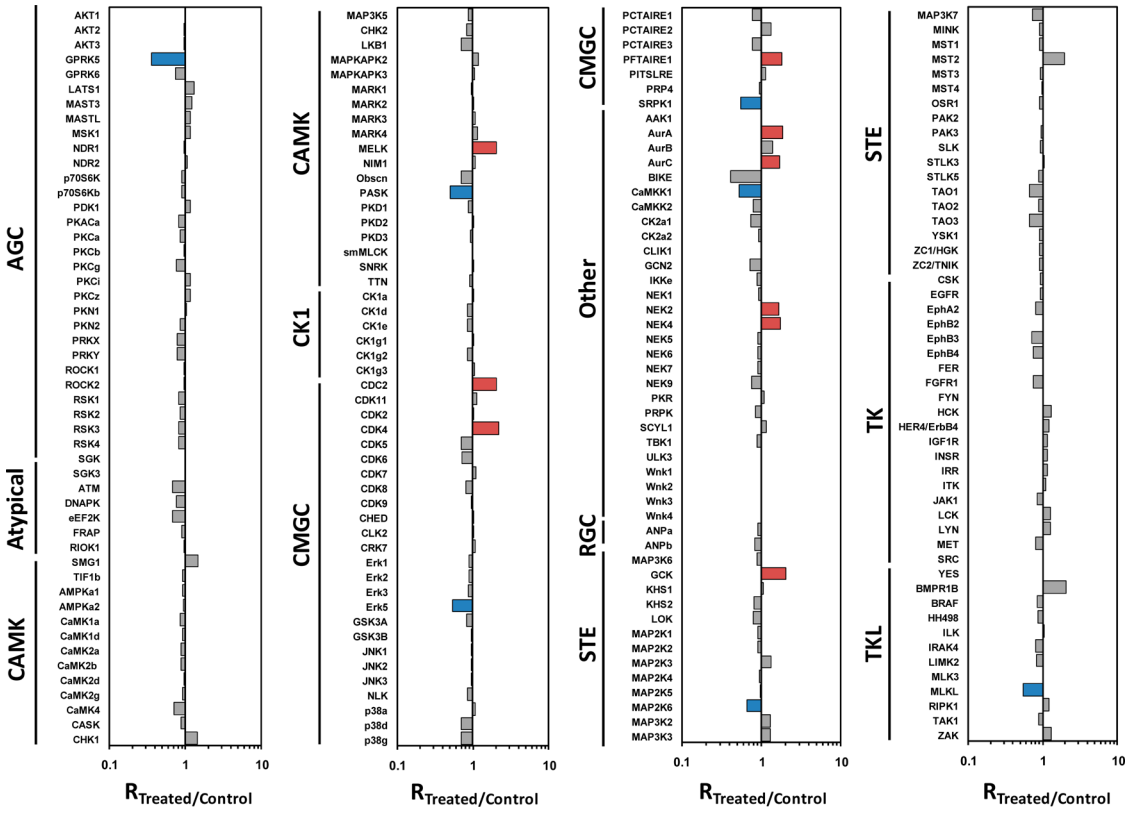

Figure 4. Global kinome profiling for GM00637 human skin fibroblasts after treatment with 5 μM sodium arsenite for 24 h. Blue and red bars denote kinases that are down- and up-regulated after sodium arsenite exposure, respectively.

Scheduled MRM Analysis with On-the-Fly Correction of Retention Time Shift. To achieve large-scale global kinome analysis for more than 300 kinases, it is essential to perform scheduled MRM analysis, which necessitates accurate prediction of retention time. In our previous workflow, we predicted the retention time for individual peptides based on their empirically determined iRT scores.[13] However, a wide variety of factors can give rise to retention time variations. For example, sample loading, difference in column packing, instabilities of LC systems, and mobile phase flow rate can all lead to an unexpected shift in retention time, which decreases the reproducibility and accuracy for quantification by scheduled MRM analysis. In our previous experiment, although the targeted kinase peptides follow strictly the elution order according to their iRT scores, we also observed a 2−3 min delay in retention time after multiple sample injections, which may result in the failure of detecting some kinase peptides if a narrow detection window is imposed in the scheduled MRM analysis.

To correct for systematic retention time shift during the scheduled LC-MRM analysis, we incorporated an on-the-fly correction[16,17] in our MRM detection workflow, during which the instrument automatically detects the shift in retention time for predefined reference peptides and adjusts, in real-time, the retention time window for subsequently eluted targeted peptides. Since this recalibration of retention time occurred in real-time, it could greatly reduce the chance of peak loss arising from the retention time shift during scheduled MRM analysis. In our test experiment for monitoring the tryptic digestion mixture of BSA, we found that peptides with large retention time shift can still be successfully captured with the on-the-fly technique. For instance, Figure 3A shows the chromatograms for two peptides (AEFVEVTK and LGEYGFQNALIVR) from tryptic digestion mixture of BSA. With an intentionally delayed gradient, the actual retention times of these two peptides were postponed by 9 and 8 min, respectively, from previous LC-MRM runs. Thus, without the on-the-fly correction of retention time shift, the transitions of these two peptides would not be captured in the predicted retention time window. However, using the same detection windows, these two BSA peptides with very large retention time shifts can still be successfully detected with the real-time adjustment of the detection window. Therefore, the on-the-fly technique is expected to easily correct for the retention time shift observed in our kinome MRM analysis, which generally lies within the 2−3 min range.

To achieve on-the-fly recalibration of the retention time shift for our MRM-based kinome analysis, we spiked a set of commercially available standard peptides into the sample.[17] The iRT values of these reference peptides were also recalculated by coinjection with tryptic peptides of BSA, whose iRT scores are well-defined in the kinome library (Table S1, Supporting Information). In our experience, we found that employing two reference peptides as retention time markers is sufficient for systematic correction of retention time, whereas too many reference peptides may adversely affect the real-time detection window adjustment by the interference from complex sample matrices. In addition, the early eluted standard peptides, which generally have large retention time variations, were not employed as the reference peptides. Therefore, we chose the third and fourth eluted standard peptides IGDYAGIK and TASEFDSAIAQDK as the reference peptides for on-the-fly corrections, and the detection time window was set at 16 min so that no reference could be missed even with large retention

dx.doi.org/10.1021/ac502592d | Anal. Chem. 2014, 86, 10700−10707

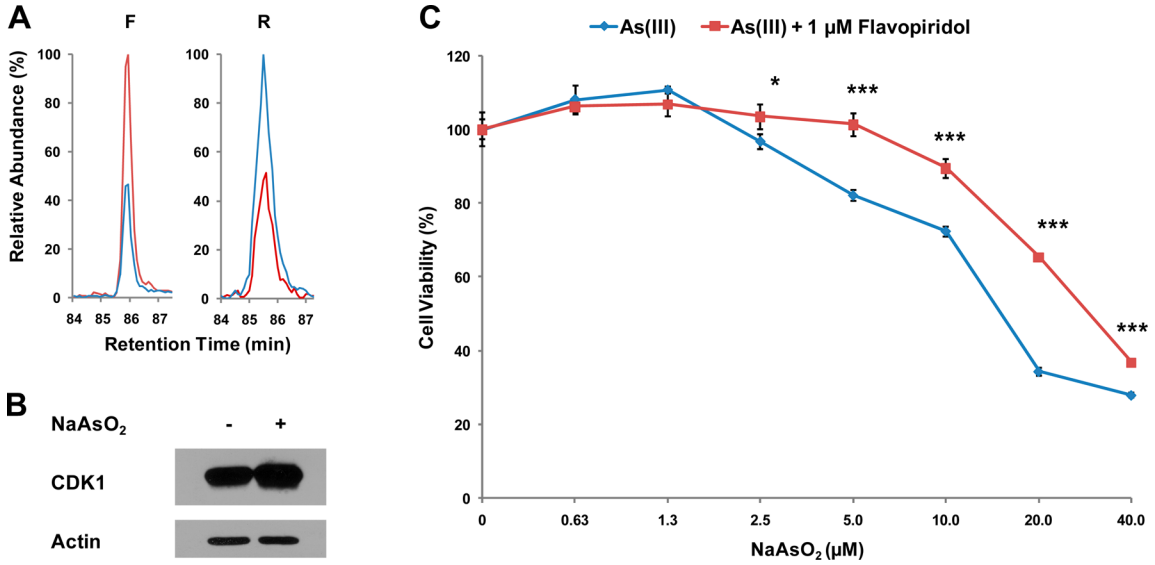

Figure 5. Sodium arsenite-induced elevated expression of cyclin-dependent kinase 1 (CDK1) (A, B) and arsenite-induced growth inhibition of cells can be rescued by a CDK inhibitor, flavopiridol (C). (A) Quantitative results by LC-MRM analysis for peptide DLK*PQNLLIDDK ("K*" designates the desthiobiotin-labeled lysine) from CDK1. Shown are the extracted-ion chromatograms for three transitions monitored for the peptide with light (red) and heavy (blue) labels in forward (left) and reverse (right) SILAC experiments. (B) Western blot analysis revealed the elevated expression of CDK1 upon arsenite treatment. (C) The MTT assay showed that flavopiridol could significantly restore the cell proliferation rate after sodium arsenite treatment. "*", $p < 0.05$; "**", $p < 0.01$; "***", $p < 0.001$. The p values were calculated by using an unpaired two-tailed t test. The values represent the mean of results obtained from three independent experiments.

time shift. As a result, the detection window for subsequently eluted target peptides will be adjusted according to a linear fit through the predicted and actual RTs of reference peptides IGDYAGIK and TASEFDSAIAQDK. Owing to this on-the-fly adjustment and the resultant increased accuracy in retention time prediction, the duration of the retention time window could be shortened from 10 min, as used in our previous study,[13] to 6 min. As depicted in Figure 3B, for monitoring a total of more than 2000 transitions with a 10 min scheduled retention time window, four LC-MRM analytical runs are required since the maximum capacity for LC-MRM analysis is around 170 transitions per cycle. With a 6 min retention time window, the MS was capable of monitoring the same number of transitions in 2 scheduled LC-MRM runs. Thus, this method improved the analytical throughput, reduced the amount of analyte required, and increased the analytical robustness and accuracy.

Sodium Arsenite-Induced Perturbation of the Entire Kinome. Previously, we utilized the isotope-coded ATP affinity probes in conjunction with the scheduled MRM analysis to achieve a comparative analysis of the global kinome of a pair of melanoma cell lines derived from the primary (WM-115) and metastatic (WM-266-4) tumor sites of the same individual.[13] However, this targeted MRM analysis was not applied to study the global kinome response upon external chemical stimulus, which has broad applications in research in cell signaling and environmental toxicology. Therefore, in the current study, we further expanded the application of this technique to elucidate, with the use of an SILAC-based approach, the perturbation of the entire kinome induced by an environmental toxicant, sodium arsenite. In the same vein, exposure to arsenic species in drinking water is a widespread public health concern worldwide. Researchers from disparate fields have explored the mechanisms of action of arsenic species from different perspectives, ranging from speciation to metabolism.[24,25] Owing to the importance of kinases in cell signaling, we decided to employ the MRM-based method to conduct an in-depth profiling of the alteration of global kinome in human cells in response to sodium arsenite exposure.

GM00637 human skin fibroblast cells were treated with 5 μM sodium arsenite [iAs(III)] for 24 h. The subsequent ATP affinity probe labeling and sample preparation were as described in Figure 1B. The resulting enriched kinase peptides were analyzed by two scheduled MRM runs with a 6 min retention time window and on-the-fly retention time correction strategy. In total, we quantified 234 kinases from one forward and two reverse SILAC experiments (Table S3, Supporting Information). In addition, the excellent correlation between the measured retention time with iRT demonstrated the effectiveness of this strategy (Figure 3C). Depicted in Figure 4 is the histogram of kinome quantification results, which revealed that kinases from all kinase groups except the PKL group were quantified. Although the expression levels and ATP binding affinities of the majority of the kinases in the kinome remained unchanged toward iAs(III) treatment, 8 and 9 kinases were significantly down- and up-regulated, respectively (Figures 4 and S1 and S2 and Table S2, Supporting Information).

It is worth discussing the analytical performances of the MRM-based kinome profiling method. As noted in our recent study,[13] the MRM-based targeted proteomic approach affords better sensitivity, reproducibility, and coverage for global kinome analysis than the short-gun proteomic approach. In addition, we observed that the MRM-based method provided an excellent dynamic range for kinome quantification. Signal intensities, as reflected by peak areas found in the selected-ion chromatograms for MRM transitions, vary from 10^3 to 10^6 (Figure S3, Supporting Information). Thus, kinases with expression levels differing by 2 to 3 orders of magnitude can be simultaneously monitored and quantified. Second, to achieve high specificity in the MRM-based kinome analysis, we chose only those kinase peptides that are directly associated with ATP binding or possess known ATP-binding motifs (HRDxKxxN,

dx.doi.org/10.1021/ac502592d | Anal. Chem. 2014, 86, 10700−10707

VAxK, or GxxxxGK) for the construction of the kinome MRM library.[13] As a result, quantifications of the majority of kinases were based on single unique peptides. Nevertheless, 66 out of the 234 kinases were quantified on the basis of multiple peptides. Quantitative variations among the multiple unique peptides for any of the 66 kinases are relatively small, as manifested by an average relative standard deviation (RSD) of 12.6% (calculated on the basis of data shown in Table S3, Supporting Information).

Sodium Arsenite Exposure Induced Hyperactivation of Cyclin-Dependent Kinase 1 and Other Cell Cycle-Related Protein Kinases. Different mechanisms were proposed about how arsenic species exert their cytotoxic effects, which include induction of oxidative stress and dysfunction of proteins through binding to vicinal thiol groups.[26] Especially, cell cycle arrest induced by inorganic arsenic exposure has been observed by multiple research groups.[27]

In the current study, we observed the overexpression of multiple protein kinases associated with cell cycle progression. For instance, we observed an elevated level of cyclin-dependent kinase 1 (CDK1) in both forward and reverse SILAC experiments (ratio of 2.07, Figures 5A and S2, Supporting Information). Along this line, our Western blot analysis independently confirmed the increased expression of CDK1, as illustrated in Figure 5B. In agreement with our observation, cDNA microarray analysis also revealed the augmented expression of CDK1 in sodium arsenite-treated HFW human fibroblast cells.[28]

CDK1 plays pivotal roles in regulating mammalian cell cycle progression, which is an evolutionarily conserved and highly regulated process. Sustained activation of CDK1 was found to arrest cells in the metaphase and cause mitotic failure which eventually induces cell death.[29] In this vein, hyperactivation of CDK1 was observed to induce mitotic arrest in A375 leukemia cells after arsenite exposure.[30] Thus, aberrant hyperactivation of CDK1 may account, in part, for the cytotoxicity of sodium arsenite, and inhibition of CDK1 may result in a decreased sensitivity toward sodium arsenite exposure. To test this hypothesis, we cotreated GM00637 cells with sodium arsenite and an effective CDK inhibitor, flavopiridol,[31] and monitored the proliferation of the cells using the MTT assay. Our results showed that treatment with flavopiridol rescued in part the arsenite-induced growth inhibition (Figure 5C). Therefore, inhibition of CDK1 hyperactivities could reduce the cytotoxicity of sodium arsenite in human skin fibroblasts.

Apart from CDK1, we found that arsenite exposure also led to the up-regulation of several other kinases involved in cell cycle progression. In this vein, we observed elevated levels of all three members of Aurora kinases (AurA, AurB, and AurC) by 1.85-, 1.37-, and 1.68-fold, respectively, following arsenite treatment. Aurora kinases play vital roles in regulating cell cycle progression. Different members of Aurora kinases possess distinct functions and subcellular localizations; however, there is partial overlap and coordination of their functions.[32] AurA is implicated in centrosome segregation and spindle assembly, and it controls the transition between different phases of the cell cycle, whereas AurB is involved in chromatin modification, spindle checkpoint signaling, and cytokinesis.[33,34] The function of AurC is ambiguous owing to the paucity of studies; however, it may serve as a potential chromosomal passenger protein as AurB and regulate spindle checkpoint.[35] Overexpression of Aurora kinases has been linked to centrosome amplification, multinuclei formation, and aneuploidy.[36] The activation of individual Aurora kinases upon arsenite treatment was observed previously. For example, AurA was found to be elevated in immortalized keratinocytes upon treatment with a low dose (<1 μM) of arsenite.[37] Likewise, AurB was found to be increased in Hela-S3 cells upon exposure with arsenic trioxide.[38] Here, facilitated by this global kinome analysis technique, we demonstrated unambiguously the global elevated expression/activation for all three Aurora kinases upon arsenite treatment, which may induce cell cycle dysregulation. Thus, the aberrant expression and activation of cell cycle-related kinases and the ensuing perturbation in mitotic progression may account, in part, for the cytotoxic and carcinogenic effects of arsenite.

CONCLUSIONS

Maturation of the targeted proteomic approach provides a solid foundation for global kinome profiling. By interrogating this important family of enzymes, more information can be garnered on the details of critical cellular processes, such as cell signaling and cell proliferation. In the present study, a reactive ATP affinity probe, coupled with SILAC labeling and scheduled MRM analysis, was harnessed for global kinome profiling. By adopting "on-the-fly" recalibration of retention time shift with "spiked-in" reference peptides to the targeted kinome analysis, we were able to shorten the duration of the retention time window from 10 to 6 min. In doing so, ~2000 transitions of ~400 kinase peptides can be monitored in two LC-MRM runs without compromising the overall analytical performance. By taking advantage of the above-described method, we achieved, for the first time, an in-depth analysis of arsenic-induced global kinome perturbation in GM00637 human skin fibroblasts. This further demonstrated that the ATP affinity labeling method is amenable to both chemical and metabolic labeling, and the method is also powerful for exploring the disturbance in the cell signaling network in response to environmental toxicant exposure.

A total of 245 unique peptides, representing 234 unique kinases, was quantified from three independent SILAC experiments. Several kinases involved in cell cycle progression were found to be hyperactivated. Among them, the expression level of CDK1 was increased by ~2-fold, which was further confirmed by Western analysis. Additionally, treatment with a CDK1 inhibitor, flavopiridol, could partly rescue the cells from arsenite-induced growth inhibition. Thus, we reason that sodium arsenite may exert its cytotoxic effect, in part, through aberrant activation of CDK1 and the resultant disturbance of cell cycle progression. In addition, other kinases involved in the mitotic progression, including Aurora kinases, were found to be activated, which may give rise to mitotic instability and, eventually, cell death. Together, the above findings strongly support that MRM- and ATP affinity probe-based kinome profiling constitutes a powerful tool for the discovery of molecular mechanisms of action of environmental toxicants.

ASSOCIATED CONTENT

Supporting Information

List of reference peptides, details of peptides and kinases quantified in scheduled MRM analysis, representative LC-MS/MS data, and Skyline file for SILAC-compatible MRM kinome library. This material is available free of charge via the Internet at http://pubs.acs.org.

AUTHOR INFORMATION

Corresponding Author

*E-mail: yinsheng.wang@ucr.edu. Telephone: (951) 827-2700. Fax: (951) 827-4713.

Notes

The authors declare no competing financial interest.

ACKNOWLEDGMENTS

This work was supported by the National Institutes of Health (R01 ES019873).

REFERENCES

(1) Cheng, H. C.; Qi, R. Z.; Paudel, H.; Zhu, H. J. *Enzyme Res.* **2011**, *2011*, 794089.
(2) Johnson, L. N. *Biochem. Soc. Trans.* **2009**, *37*, 627−641.
(3) Lahiry, P.; Torkamani, A.; Schork, N. J.; Hegele, R. A. *Nat. Rev. Genet.* **2010**, *11*, 60−74.
(4) Carpenter, R. L.; Jiang, B. H. *Curr. Cancer Drug Targets* **2013**, *13*, 252−266.
(5) Stains, C. I.; Tedford, N. C.; Walkup, T. C.; Luković, E.; Goguen, B. N.; Griffith, L. G.; Lauffenburger, D. A.; Imperiali, B. *Chem. Biol.* **2012**, *19*, 210−217.
(6) Houseman, B. T.; Huh, J. H.; Kron, S. J.; Mrksich, M. *Nat. Biotechnol.* **2002**, *20*, 270−274.
(7) Mann, M. *Nat. Rev. Mol. Cell Biol.* **2006**, *7*, 952−958.
(8) Tao, W. A.; Wollscheid, B.; O'Brien, R.; Eng, J. K.; Li, X. J.; Bodenmiller, B.; Watts, J. D.; Hood, L.; Aebersold, R. *Nat. Methods* **2005**, *2*, 591−598.
(9) Daub, H.; Olsen, J. V.; Bairlein, M.; Gnad, F.; Oppermann, F. S.; Körner, R.; Greff, Z.; Kéri, G.; Stemmann, O.; Mann, M. *Mol. Cell* **2008**, *31*, 438−448.
(10) Patricelli, M. P.; Szardenings, A. K.; Liyanage, M.; Nomanbhoy, T. K.; Wu, M.; Weissig, H.; Aban, A.; Chun, D.; Tanner, S.; Kozarich, J. W. *Biochemistry* **2007**, *46*, 350−358.
(11) Xiao, Y.; Guo, L.; Jiang, X.; Wang, Y. *Anal. Chem.* **2013**, *85*, 3198−3206.
(12) Olsen, J. V.; Schwartz, J. C.; Griep-Raming, J.; Nielsen, M. L.; Damoc, E.; Denisov, E.; Lange, O.; Remes, P.; Taylor, D.; Splendore, M.; Wouters, E. R.; Senko, M.; Makarov, A.; Mann, M.; Horning, S. *Mol. Cell. Proteomics* **2009**, *8*, 2759−2769.
(13) Xiao, Y.; Guo, L.; Wang, Y. *Mol. Cell. Proteomics* **2014**, *13*, 1065−1075.
(14) MacLean, B.; Tomazela, D. M.; Shulman, N.; Chambers, M.; Finney, G. L.; Frewen, B.; Kern, R.; Tabb, D. L.; Liebler, D. C.; MacCoss, M. J. *Bioinformatics* **2010**, *26*, 966−968.
(15) Picotti, P.; Aebersold, R. *Nat. Methods* **2012**, *9*, 555−566.
(16) Escher, C.; Reiter, L.; MacLean, B.; Ossola, R.; Herzog, F.; Chilton, J.; MacCoss, M. J.; Rinner, O. *Proteomics* **2012**, *12*, 1111−1121.
(17) Kiyonami, R.; Schoen, A.; Zabrouskov, V. *On-the-Fly Retention Time Shift Correction for Multiple Targeted Peptide Quantification by LC-MS/MS*; Thermo Fisher Scientific, Application Note 503; Thermo Fisher Scientific, Inc.: San Jose, CA, 2010.
(18) Chen, X.; Smith, L. M.; Bradbury, E. M. *Anal. Chem.* **2000**, *72*, 1134−1143.
(19) Zhu, H.; Pan, S.; Gu, S.; Bradbury, E. M.; Chen, X. *Rapid Commun. Mass Spectrom.* **2002**, *16*, 2115−2123.
(20) Ong, S. E.; Blagoev, B.; Kratchmarova, I.; Kristensen, D. B.; Steen, H.; Pandey, A.; Mann, M. *Mol. Cell. Proteomics* **2002**, *1*, 376−386.
(21) Guo, L.; Xiao, Y.; Wang, Y. *Toxicol. Appl. Pharmacol.* **2014**, *277*, 21−29.
(22) Guo, L.; Xiao, Y.; Wang, Y. *J. Proteome Res.* **2013**, *12*, 3511−3518.
(23) Xiao, Y.; Guo, L.; Wang, Y. *Anal. Chem.* **2013**, *85*, 7478−7486.
(24) Watanabe, T.; Hirano, S. *Arch. Toxicol.* **2013**, *87*, 969−979.
(25) Planer-Friedrich, B.; Suess, E.; Scheinost, A. C.; Wallschlager, D. *Anal. Chem.* **2010**, *82*, 10228−10235.
(26) Shen, S.; Li, X. F.; Cullen, W. R.; Weinfeld, M.; Le, X. C. *Chem. Rev.* **2013**, *113*, 7769−7792.
(27) McCollum, G.; Keng, P. C.; States, J. C.; McCabe, M. J., Jr. *J. Pharmacol. Exp. Ther.* **2005**, *313*, 877−887.
(28) Yih, L. H.; Peck, K.; Lee, T. C. *Carcinogenesis* **2002**, *23*, 867−876.
(29) Castedo, M.; Perfettini, J.-L.; Roumier, T.; Andreau, K.; Medema, R.; Kroemer, G. *Oncogene* **2004**, *23*, 2825−2837.
(30) McNeely, S. C.; Taylor, B. F.; States, J. C. *Toxicol. Appl. Pharmacol.* **2008**, *231*, 61−67.
(31) Shapiro, G. I. *Clin. Cancer Res.* **2004**, *10*, 4270s−4275s.
(32) Hochegger, H.; Hégarat, N.; Pereira-Leal, J. B. *Open Biol.* **2013**, *3*, 120185.
(33) Santaguida, S.; Vernieri, C.; Villa, F.; Ciliberto, A.; Musacchio, A. *EMBO J.* **2011**, *30*, 1508−1519.
(34) Nikonova, A. S.; Astsaturov, I.; Serebriiskii, I. G.; Dunbrack, R. L., Jr.; Golemis, E. A. *Cell. Mol. Life Sci.* **2013**, *70*, 661−687.
(35) Sasai, K.; Katayama, H.; Stenoien, D. L.; Fujii, S.; Honda, R.; Kimura, M.; Okano, Y.; Tatsuka, M.; Suzuki, F.; Nigg, E. A.; Earnshaw, W. C.; Brinkley, W. R.; Sen, S. *Cell Motil. Cytoskeleton* **2004**, *59*, 249−263.
(36) Fu, J.; Bian, M.; Jiang, Q.; Zhang, C. *Mol. Cancer Res.* **2007**, *5*, 1−10.
(37) Wu, C. H.; Tseng, Y. S.; Kao, Y. T.; Sheu, H. M.; Liu, H. S. *Toxicol. Sci.* **2013**, *132*, 43−52.
(38) Yih, L. H.; Hsu, N. C.; Wu, Y. C.; Yen, W. Y.; Kuo, H. H. *Toxicol. Appl. Pharmacol.* **2013**, *267*, 228−237.